Supplementary Information (SI) for Journal of Materials Chemistry A.
This journal is © The Royal Society of Chemistry 2025

Supporting Information

In-situ grown $ZnIn_2S_4$ on $Zn_2SiO_4:Ga^{3+}$ core-shell heterojunction for photocatalytic hydrogen production

Wenchao Wei, Mamutjan Tursun, Peng Yan, Aikelaimu Aihemaiti, and Abdukader Abdukayum*

Xinjiang Key Laboratory of Novel Functional Materials Chemistry, College of Chemistry and Environmental Sciences, Kashi University, Kashgar 844000, China

*Corresponding authors: Prof. Dr. A. Abdukayum (E-mail: abdukadera@sina.com

Contents

Experimental materials

Zinc nitrate ($Zn(NO_3)_2·9H_2O$), gallium nitrate ($Ga(NO_3)_3$), citric acid, tetraethoxysilane, indium chloride ($InCl_3$), zinc chloride ($ZnCl_2$), Thioacetamide (TAA), glycerol, absolute alcohol, Deionized (DI) water, sodium sulfide nonahydrate ($Na_2S·9H_2O$), sodium sulfite (Na_2SO_3), and chloroplatinic acid were purchased from Aladdin Bio-Chem Technology Co. All reagents used in this study were analytically pure reagents and did not require further processing.

Synthesis of Zn_2SiO_4:Ga^{3+}

In a typical method, 29.748g of $Zn(NO_3)_2·9H_2O$(100mmol), 0.2557g of $Ga(NO_3)_3$(1mmol), and 42.028g of citric acid were combined in 200ml of deionized (DI) water. Subsequently,50mmol tetraethoxysilane was added to the mixed solution. The mixture was agitated for ten minutes, after which it underwent a drying process at a temperature of 80 ℃ for 24 hours. The resulting dry gel was then subjected to annealing at 600 ℃ for 2 hours, followed by cooling and milling. A second annealing process was conductedat 1000 ℃ for 2 hours. After milling, Zn_2SiO_4:Ga^{3+} was obtained.

Synthesis of $ZnIn_2S_4$

A total of 0.055 g of $ZnCl_2$, 0.177 g of $InCl_3$, and 0.24g of TAA were dissolved in 40 mL of deionized water containing 20 vol% glycerol, and the mixture was stirred for 0.5 hours. Subsequently, the solution was subjected to stirring and reacted in an oil bath at 80℃ for 2 hours. After the reaction, the mixture was allowed to cool to room temperature, and the products were washed three times with DI water and anhydrous ethanol. Finally, the products were dried at 60 ℃ overnight to obtain $ZnIn_2S_4$.

Synthesis of Zn_2SiO_4:Ga^{3+}@$ZnIn_2S_4$

A certain amount of Zn_2SiO_4:Ga^{3+} was ultrasonically dispersed into 40 ml of aqueous solution containing 20 vol% glycerol for 0.5 h. Subsequently,0.055 g of $ZnCl_2$, 0.177 g of $InCl_3$, and 0.24g of TAA were added to the solution, which was then stirred for an additional half an hour. Finally, the resulting solution was stirred and reacted in an oil bath at 80 ℃ for 2 h. The obtained product was washed three times with water and anhydrous ethanol, then dried overnight at 60 ℃. The synthesized samples were designated as Zn_2SiO_4:Ga^{3+}-x@ $ZnIn_2S_4$, where x represents the mass (mg) of Zn_2SiO_4:Ga^{3+}, with values of x being 0, 5, 10, 20, 40, and 80.

Characterization

The samples were then analyzed for their crystal structures using a Bruker D8 ADVANCE X-ray diffractometer; The morphology of the samples was observed through scanning electron microscopy (SEM, ZEISS Sigma 300, Germany) and field emission transmission electron microscopy (TEM, Hitachi HT7820, Japan). Spectra of the samples were collected in therange of 300-800 nm and band gaps were calculated using a Hitachi UH1450 ultraviolet-visible (UV-vis) spectrophotometer. The surface chemical state and composition of the samples were analyzed via X-ray photoelectron spectroscopy (XPS, Thermo Scientific K-Alpha, USA). Additionally, thespecific surface area and pore size of the samples were evaluated using a Micromeritics ASAP

2460 Automatic Specific Surface Area Analyzer (USA).

Photocatalytic performance test

The photocatalytic hydrogen evolution experiments were conducted in a closed reaction unit (CEL-PAEM-D8 PLUS, Beijing Zhongjiao Jinyuan Science and Technology Co., Ltd.), with the temperature maintained at 20°C using a cooling circulating water system. A total of5 mg of the synthesized photocatalyst was dispersed in 100 mL of deionized water containing $Na_2S{\cdot}9H_2O$ (0.35 M) and Na_2SO_3 (0.25 M), to which 28 μL of 1 mg/mL H_2PtCl_6 was added as a co-catalyst. Before initiating the reaction, the reactor was evacuated, and the recirculating cooling system ensured a stable temperature of 20°C throughout the process. Gas samples were extracted every 1 hour under irradiation from a 300 W xenon lamp (CEL-HXF300-T3), and hydrogen production was analyzed using a gas chromatograph (GC-7920) equipped with a 5 Å molecular sieve column and a thermal conductivity detector (TCD).

The apparent quantum efficiencies (AQEs) for photocatalytic H_2 evolution was measured using different monochromatic light filters (365, 400, 420nm), and the AQEs were calculated according to the following equation[1]:

$$AQEs(\%) = \frac{2 \times number\ of\ evolved\ H_2\ molecules}{number\ of\ incident\ photons} \times 100\%$$

$$= \frac{2 \times n_{H_2} \times N_A \times h \times c}{S \times P \times t \times \lambda}$$

where n_{H_2} is the amount of H_2 molecules, N_A is the Avogadro constant, h is the Planck constant, c is the speed of light, S is the irradiation area, P is the intensity of irradiation light which is measured by an optical power meter (CEL-NP2000, CEAU-LIGHT Co., Ltd.), t is the photoreaction time, and λ represents the wavelength of monochromatic light.

Photoelectrochemical test

2 mg of the photocatalyst powder was dispersed in a mixed solution containing 800 μL of deionized water, 150 μL of ethanol, and 50 μL of perfluorosulfonic acid. This mixture was ultrasonically dispersed for 30 min, after which it was dried by depositing it onto a conductive glass substrate. In the electrochemical workstation (Chenhua CHI760E, China), a 300W Xe lamp was used as the light source, while a 0.1 M Na_2SO_4 aqueous solution was utilized as the electrolyte. The photocurrent response curves, electrochemical impedance spectra (EIS), and Mott-Schottky plots were recorded using a three-electrode system which included a Pt plate as the auxiliary electrode, an Ag/AgCl electrode as the reference electrode, and the prepared conductive glass as the working electrode.

Computational methods

The DFT calculations were performed using the Vienna Ab Initio Simulation Package (VASP) with the Perdew-Burke-Enzerhof (PBE) functional within the generalised gradient approximation (GGA) and selecting the projector augmented wave (PAW) pseudopotentials [2–4] . A plane wave basis set with a cutoff energy of 450 eV was utilized. All calculations were spin

polarised. To sample the Brillouin zone, Monkhorst-Pack k-point grids of 2 × 2 × 3 were selected for the $ZnIn_2S_4$ and $Zn_2SiO_4:Ga^{3+}$ bulk materials. For the slab with a p(3 ×3) $ZnIn_2S_4$ supercell and the $ZnIn_2S_4$- $Zn_2SiO_4:Ga^{3+}$ heterojunction slab, the Brillouin zone was sampled using 3 × 3 × 1 k points in the Monkhorst-Pack scheme.[5].All atoms underwent a full relaxation process without any constraints, ensuring that the energy and residual force were converged to 10^{-4} eV and 0.02 eV $Å^{-1}$, respectively.The D3-Grimme correction (DFT-D3) was used to describe the van der Waals (vdW) interactions[6] in calculating the adsorption energy of H.

Table S1. Specific surface area void parameters for $Zn_2SiO_4:Ga^{3+}$, $ZnIn_2S_4$, $Zn_2SiO_4:Ga^{3+}$-40@ $ZnIn_2S_4$

Sample	Surface area (BET) S/($m^2 \cdot g^{-1}$)	Pore diameter (D/nm)	Pore volume (BJH) V/($cm^3 \cdot g^{-1}$)
$ZnIn_2S_4$	169.9819	8.2962	0.381142
$Zn_2SiO_4:Ga^{3+}$	1.7230	11.5809	0.002558
$Zn_2SiO_4:Ga^{3+}$-40@ $ZnIn_2S_4$	176.3320	13.4996	0.630669

Table S2. List of the photocatalytic hydrogen production performance of photocatalysts in related systems

Photocatalyst	Sacrificial agent	Cocatalyst	Activity (mmol g^{-1} h^{-1})	Light source	Ref.
MIL-68(In)@$ZnIn_2S_4$	$Na_2S \cdot 9H_2O$(0.35M) Na_2SO_3(0.25M)	Pt	28.2	300 W Xe lamp	[7]
$CoS_{1.097}$@$ZnIn_2S_4$	10 vol%TEOA	-	2.6323	300 W Xe lamp (420nm>λ>780nm)	[8]
MIL-68(In)-20@$ZnIn_2S_4$	20 vol% TEOA	-	9.09	300 W Xe lamp (λ>400nm)	[9]
Co_3O_4(20) @ZIS	50%TEOA	-	5.38	300 W Xe lamp (λ>420nm)	[10]
$ZnIn_2S_4/Ti_3C_2O_x$	10%TEOA	-	0.363	300 W Xe lamp	[11]
Zv-ZIS	10%TEOA	Pt	2.65	300 W Xe lamp (λ>420nm)	[12]
$Bi_2Fe_4O_9$@$ZnIn_2S_4$	$Na_2S \cdot 9H_2O$(0.35M) Na_2SO_3(0.25M)	-	3.9643	300 W Xe lamp (λ>420nm)	[13]
$In_2O_3/ZnIn_2S_4$-5.6%	10%TEOA	Pt	2.18	300 W Xe lamp (λ>420nm)	[14]
ZMX-M	10%TEOA	Pt	14.82	300 W Xe lamp (λ>420nm)	[15]
FNS@ZIS-6	$Na_2S \cdot 9H_2O$(0.35M) Na_2SO_3(0.25M)	-	7.7	300 W Xe lamp	[16]
$Zn_2SiO_4:Ga^{3+}$-40@ $ZnIn_2S_4$	$Na_2S \cdot 9H_2O$(0.35M) Na_2SO_3(0.25M)	Pt	15.954	300 W Xe lamp	This wrok

Table S3.ICP-MS Quantitative Analysis Results for $Zn_2SiO_4:Ga^{3+}$-40@$ZnIn_2S_4$ Composite

Element	Sample Mass (g)	Content (μg kg^{-1})	Content (wt%)	Mean Content (wt%)
Ga	0.0356	1278828.251	0.13%	0.13%
	0.0356	1295639.171	0.13%	
	0.0356	1306855.211	0.13%	

Table S4. Fit parameters for the PL decay curves (Figure S7) of $ZnIn_2S_4$ and $Zn_2SiO_4:Ga^{3+}$-40@ $ZnIn_2S_4$. The lifetimes of samples can be fitted according to the dual–exponential decay kinetics: $A_1 \exp(-t/\tau_1) + A_2 \exp(-t/\tau_2)$, which can be calculated using the following expression: $\tau_{avg} = \sum A_i\tau_i^2 / \sum A_i\tau_i$, where i corresponds to the component of a given multiexponential decay process.

Samples	A_1	A_2	τ_1 (ns)	τ_2 (ns)	τ_v (ns)
$ZnIn_2S_4$	0.78539	0.1935	1.30529	7.37415	2.5049
$Zn_2SiO_4:Ga^{3+}$-40@ $ZnIn_2S_4$	0.70356	0.12863	1.77139	12.56858	3.4403

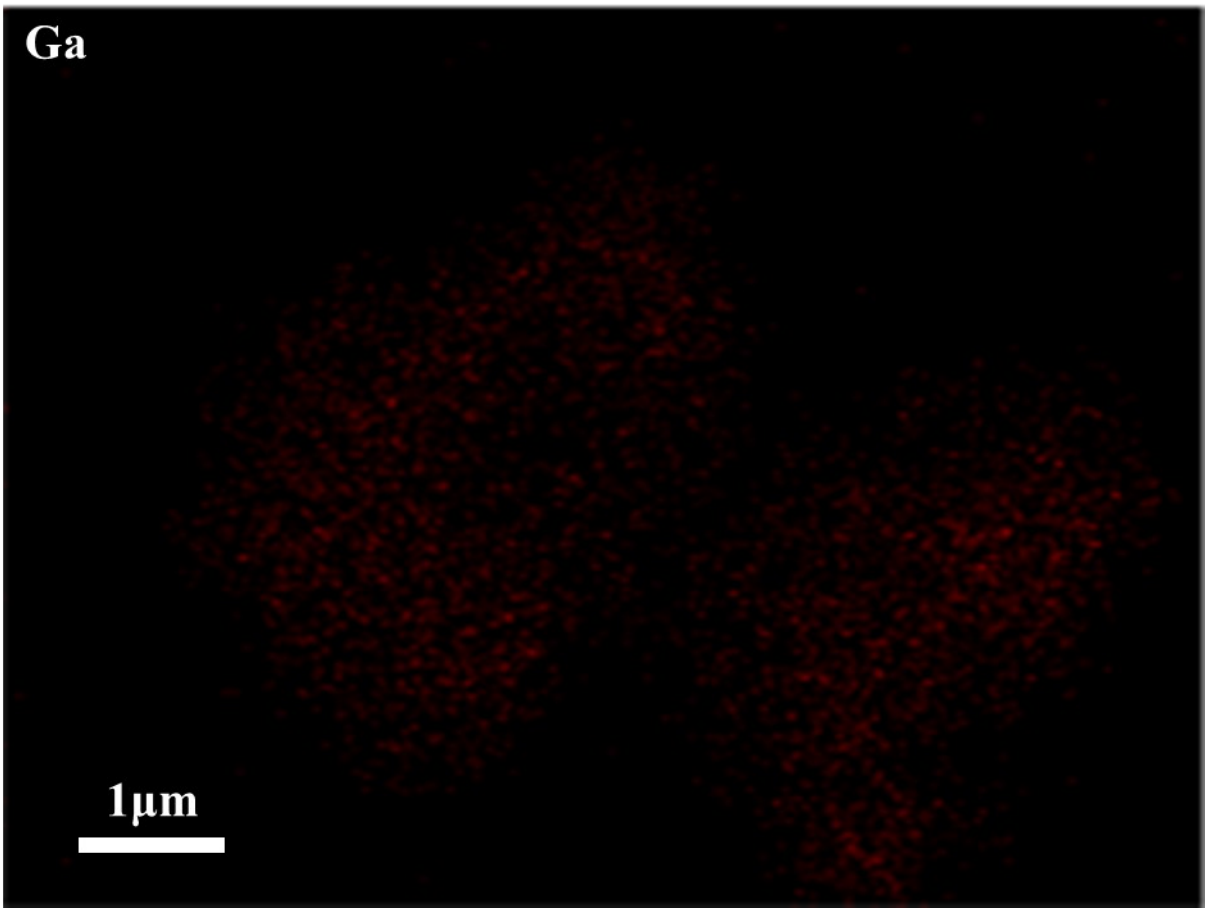

Fig. S1 The Ga elemental mappings of $Zn_2SiO_4:Ga^{3+}$-40@$ZnIn_2S_4$

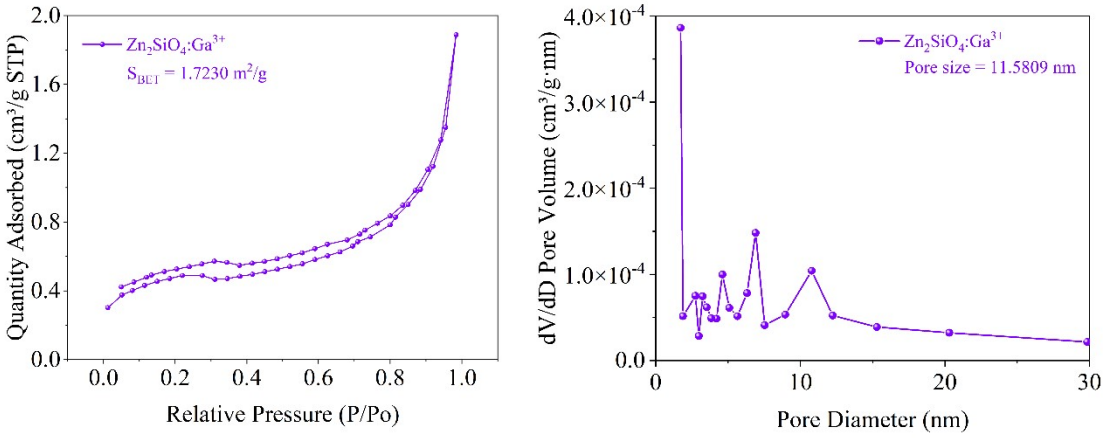

Fig. S2 Specific surface area and pore distribution for $Zn_2SiO_4:Ga^{3+}$.

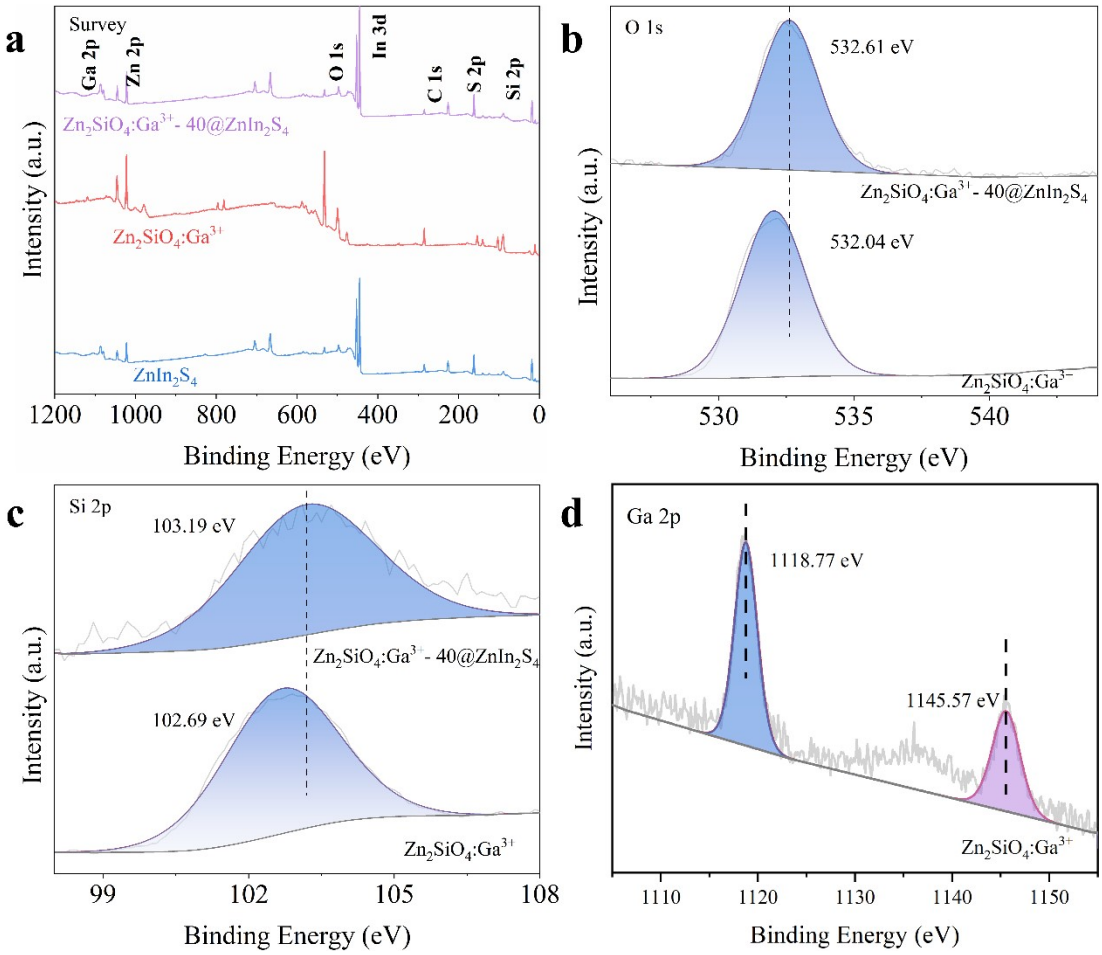

Fig. S3 The XPS spectra of $ZnIn_2S_4$, $Zn_2SiO_4:Ga^{3+}$ and $Zn_2SiO_4:Ga^{3+}$-40@ $ZnIn_2S_4$. (a) Survey (b) O1s (c) Si 2p and (d) Ga 2p

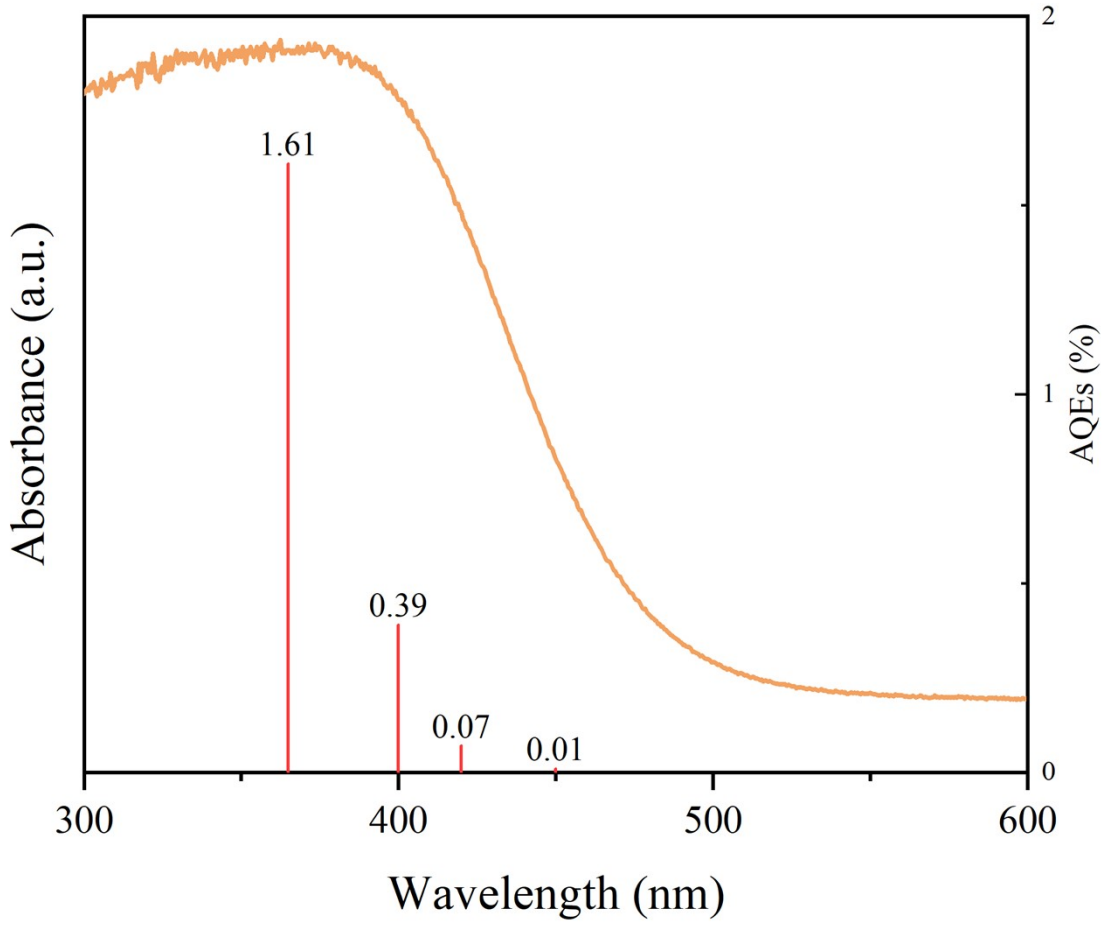

Fig. S4 AQE for Zn_2SiO_4:Ga^{3+}-40@ $ZnIn_2S_4$. at different wavelengths.

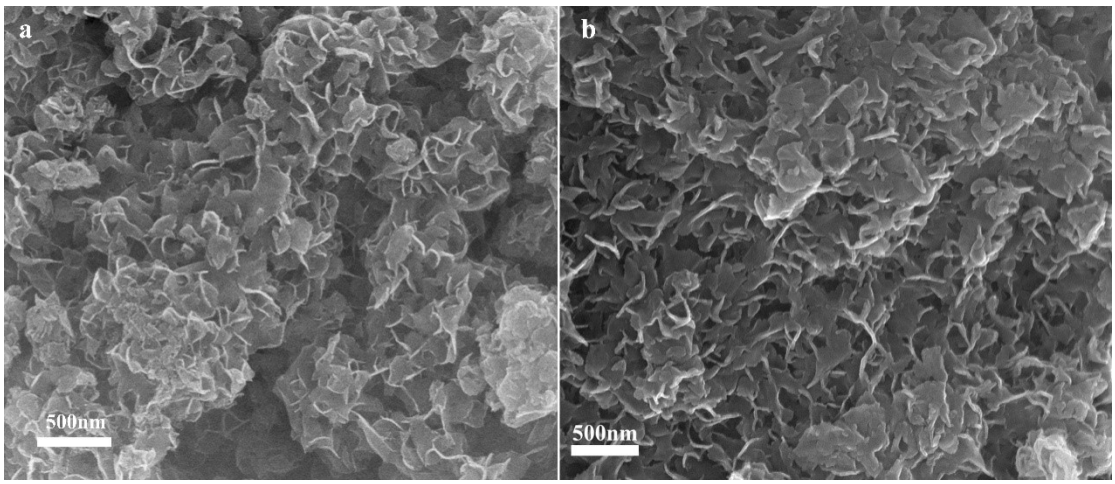

Fig. S5 SEM images of $Zn_2SiO_4:Ga^{3+}$-40@$ZnIn_2S_4$ (a) before and (b) after photocatalytic hydrogen production.

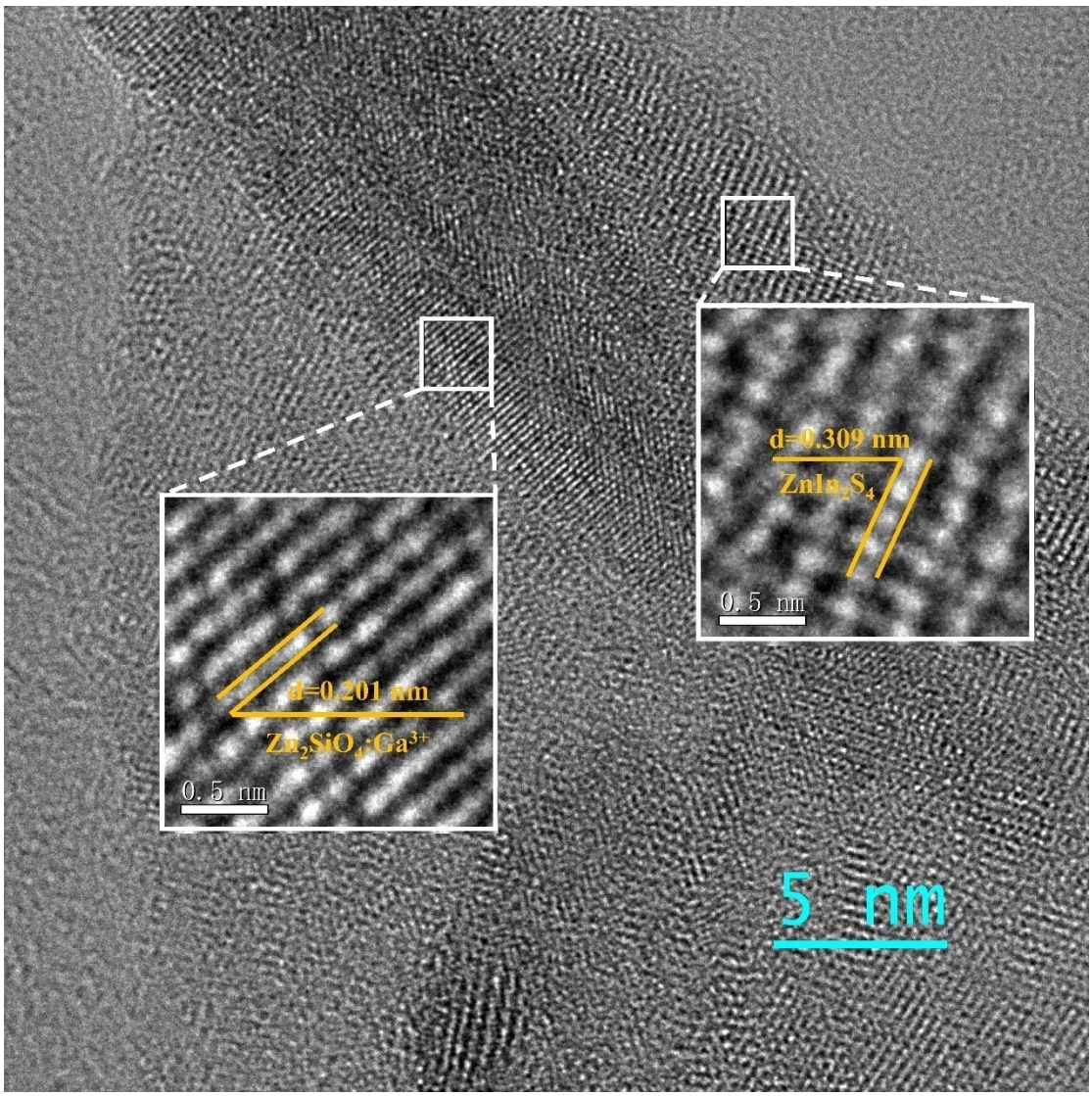

Fig. S6 HRTEM images of $Zn_2SiO_4:Ga^{3+}$-40@$ZnIn_2S_4$

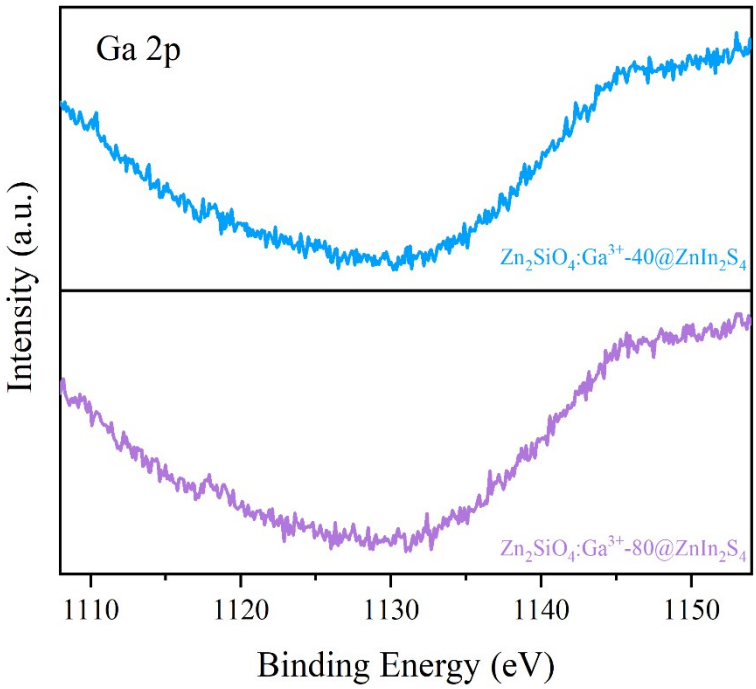

Fig. S7 The XPS spectra of $Zn_2SiO_4:Ga^{3+}$-40@ $ZnIn_2S_4$and $Zn_2SiO_4:Ga^{3+}$-80@ $ZnIn_2S_4$ Ga 2p.

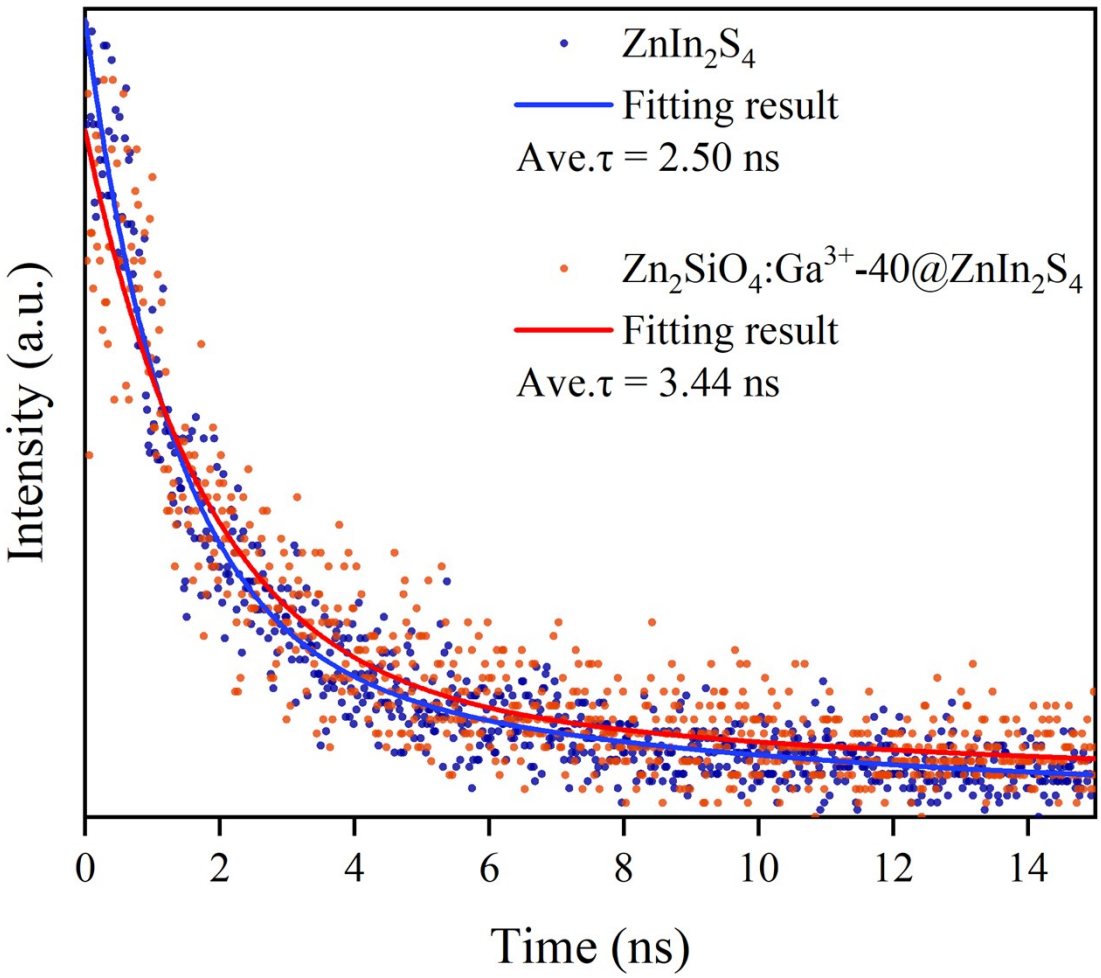

Fig. S8 Time-resolved PL spectra of $ZnIn_2S_4$ and $Zn_2SiO_4:Ga^{3+}$-40@$ZnIn_2S_4$.

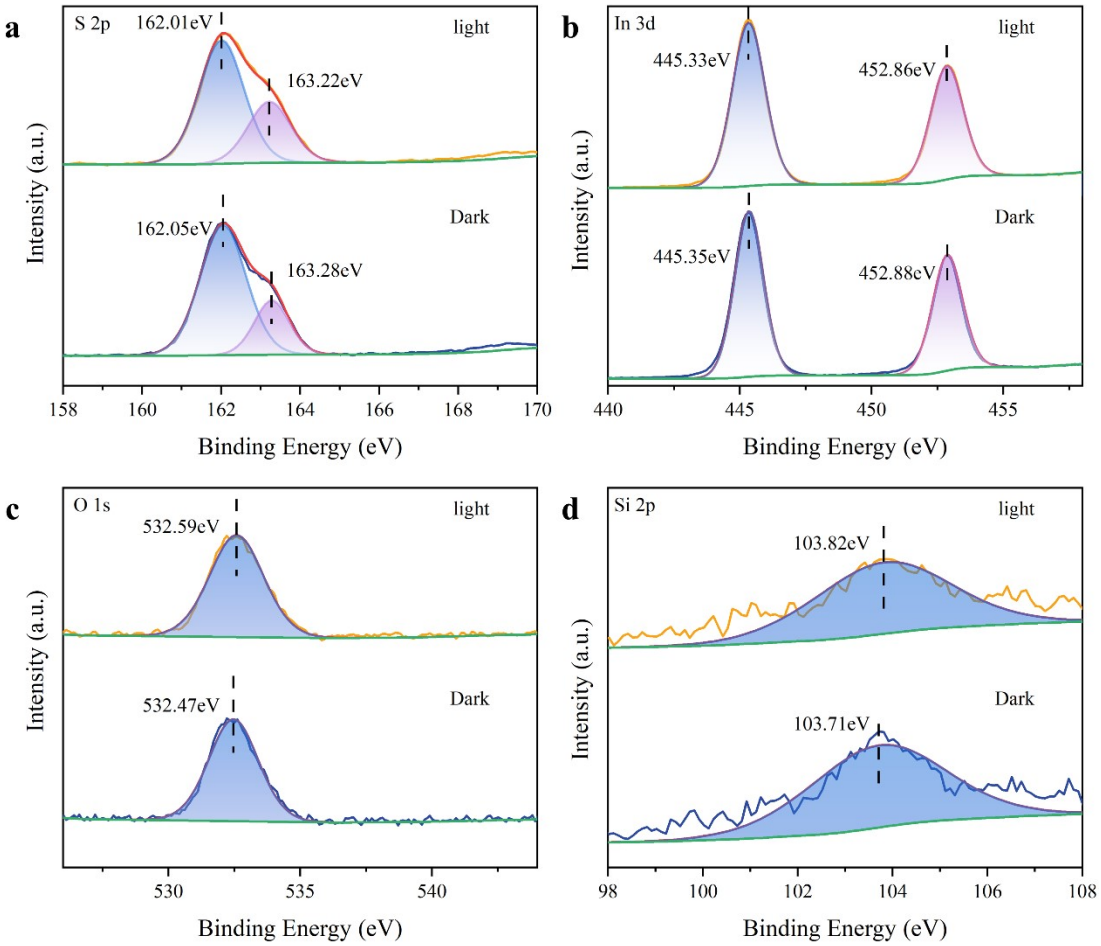

Fig. S9 High-resolution in-situ XPS spectra of S 2p(a), In 3d(b), O1s(c) and Si 2p(d) of Zn_2SiO_4:Ga^{3+}-40@$ZnIn_2S_4$.

References

[1] Q. Zhang, J. Zhang, X. Wang, L. Li, Y.-F. Li, W.-L. Dai, In–N–In Sites Boosting Interfacial Charge Transfer in Carbon-Coated Hollow Tubular $In_2O_3/ZnIn_2S_4$ Heterostructure Derived from In-MOF for Enhanced Photocatalytic Hydrogen Evolution, ACS Catal. 11 (2021) 6276–6289. https://doi.org/10.1021/acscatal.0c05520.

[2] G. Kresse, J. Furthmüller, Efficient iterative schemes for *ab initio* total-energy calculations using a plane-wave basis set, Phys. Rev. B 54 (1996) 11169–11186. https://doi.org/10.1103/PhysRevB.54.11169.

[3] J.P. Perdew, K. Burke, M. Ernzerhof, Generalized Gradient Approximation Made Simple, Phys. Rev. Lett. 77 (1996) 3865–3868. https://doi.org/10.1103/PhysRevLett.77.3865.

[4] P.E. Blöchl, Projector augmented-wave method, Phys. Rev. B 50 (1994) 17953–17979. https://doi.org/10.1103/PhysRevB.50.17953.

[5] H.J. Monkhorst, J.D. Pack, Special points for Brillouin-zone integrations, Phys. Rev. B 13 (1976) 5188–5192. https://doi.org/10.1103/PhysRevB.13.5188.

[6] S. Grimme, J. Antony, S. Ehrlich, H. Krieg, A consistent and accurate *ab initio* parametrization of density functional dispersion correction (DFT-D) for the 94 elements H-Pu, The Journal of Chemical Physics 132 (2010) 154104. https://doi.org/10.1063/1.3382344.

[7] Q. Zhang, H. Gu, X. Wang, L. Li, J. Zhang, H. Zhang, Y.-F. Li, W.-L. Dai, Robust hollow tubular $ZnIn_2S_4$ modified with embedded metal-organic-framework-layers: Extraordinarily high photocatalytic hydrogen evolution activity under simulated and real sunlight irradiation, Applied Catalysis B: Environmental 298 (2021) 120632. https://doi.org/10.1016/j.apcatb.2021.120632.

[8] X. Feng, H. Shang, J. Zhou, X. Ma, X. Gao, D. Wang, B. Zhang, Y. Zhao, Heterostructured core–shell $CoS_{1.097}@ZnIn_2S_4$ nanosheets for enhanced photocatalytic hydrogen evolution under visible light, Chemical Engineering Journal 457 (2023) 141192. https://doi.org/10.1016/j.cej.2022.141192.

[9] M. Tan, C. Yu, H. Zeng, C. Liu, W. Dong, H. Meng, Y. Su, L. Qiao, L. Gao, Q. Lu, Y. Bai, In situ fabrication of MIL-68(In)@$ZnIn_2S_4$ heterojunction for enhanced photocatalytic hydrogen production, Nanoscale 15 (2023) 2425–2434. https://doi.org/10.1039/D2NR07017K.

[10] Z. Xin, H. Zheng, J. Hu, Construction of Hollow $Co_3O_4@ZnIn_2S_4$ p-n Heterojunctions for Highly Efficient Photocatalytic Hydrogen Production, Nanomaterials 13 (2023) 758. https://doi.org/10.3390/nano13040758.

[11] M. Cai, X. Zha, Z. Zhuo, J. Bai, Q. Wang, Q. Cheng, Y. Wei, S. Sun, Enhanced Photocatalytic Hydrogen Production of $ZnIn_2S_4$ by Using Surface-Engineered $Ti_3C_2T_x$ MXene as a Cocatalyst, Materials 16 (2023) 2168. https://doi.org/10.3390/ma16062168.

[12] B. Xu, H. Li, B. Chong, B. Lin, X. Yan, G. Yang, Zn vacancy-tailoring mediated $ZnIn_2S_4$ nanosheets with accelerated orderly charge flow for boosting photocatalytic hydrogen evolution, Chemical Engineering Science 270 (2023) 118533. https://doi.org/10.1016/j.ces.2023.118533.

[13] C. Wu, Z. Xing, Y. Wang, H. Peng, W. Kong, S. Yang, Z. Li, W. Zhou, Bi2Fe4O9@ZnIn2S4 S-scheme laminated heterojunction photocatalyst towards optimized photocatalytic performance, Dalton Trans. 52 (2023) 7724–7730. https://doi.org/10.1039/D3DT01170D.

[14] P. Lu, K. Liu, Y. Liu, Z. Ji, X. Wang, B. Hui, Y. Zhu, D. Yang, L. Jiang, Heterostructure with tightly-bound interface between In_2O_3 hollow fiber and $ZnIn_2S_4$ nanosheet toward efficient visible light driven hydrogen evolution, Applied Catalysis B: Environmental 345 (2024) 123697. https://doi.org/10.1016/j.apcatb.2024.123697.

[15] M. Xu, X. Ruan, D. Meng, G. Fang, D. Jiao, S. Zhao, Z. Liu, Z. Jiang, K. Ba, T. Xie, W. Zhang, J. Leng, S. Jin, S.K. Ravi, X. Cui, Modulation of Sulfur Vacancies in ZnIn2S4/MXene Schottky Heterojunction Photocatalyst Promotes Hydrogen Evolution, (n.d.). https://doi.org/10.1002/adfm.202402330.

[16] S. Wang, D. Zhang, X. Pu, L. Zhang, D. Zhang, J. Jiang, Photothermal-Enhanced S-Scheme Heterojunction of Hollow Core–Shell FeNi2S4@ZnIn2S4 toward Photocatalytic Hydrogen Evolution, (n.d.). https://doi.org/10.1002/smll.202311504.